Electronic Supporting Information (ESI)

Probing the Dynamic Self-Assembly Behaviour of Photoswitchable Wormlike Micelles in Real Time

Elaine A. Kelly,[a] Judith E. Houston [b] and Rachel C. Evans*[c]

[a]*School of Chemistry and CRANN, University of Dublin, Trinity College, College Green, Dublin 2, Ireland.*

[b]*Jülich Centre for Neutron Science (JCNS-4), Forschungszentrum Jülich GmbH, Lichtenbergstr. 1 85748 Garching, Germany.*

[c]*Department of Materials Science and Metallurgy, University of Cambridge, 27 Charles Babbage Road, Cambridge, CB3 0FS, U.K. Email: rce26@cam.ac.uk*

Table of Contents

1. Instrumentation

1.1 Electrospray Ionisation Mass Spectrometry (ESI-MS)

ESI-MS were recorded by Dr Martin Feeney on a Bruker microTOF-Q III spectrometer interfaced to a Dionex UltiMate 3000 liquid chromatography system, in negative and positive modes as required. The instrument was calibrated using a tune mix solution (Agilent Technologies ESI-l low concentration tuning mix). Masses were recorded over the range 100-1200 *m/z*. Samples were prepared in HPLC grade solvent.

1.2 Fourier Transform Infrared (FTIR) Spectroscopy

FTIR spectra were recorded on a Perkin-Elmer Spectrum 100 FTIR spectrometer using a universal attenuated total reflection (ATR) sampling accessory. All spectra were recorded at room temperature over the range 4000-650 cm^{-1}, with a resolution of 4 cm^{-1}. The following abbreviations are used to describe the intensities: s, strong; m, medium; w, weak and br, broad.

1.3 ^{1}H and ^{13}C Nuclear Magnetic Resonance (NMR) Spectroscopy

Solution NMR spectroscopy by Dr John O'Brien was performed on a Bruker DPX 400 NMR instrument at 20 °C. ^{1}H and ^{13}C NMR spectra were obtained using an operating frequency of 400 and 151 MHz, respectively. Chemical shifts were calibrated against a tetramethylsilane (TMS) signal and are reported in parts per million (ppm). $CDCl_3$ (δ_H = 7.26 ppm, singlet; δ_C = 77.16 ppm, triplet), D_2O (δ_H = 4.79 ppm, singlet) and d_6-DMSO (δ_H = 2.50 ppm, singlet; δ_C = 39.52 ppm, septuplet) were used as deuterated solvents.

1.4 Melting Point Analysis

Measurements were performed on a Stuart SMP3 melting point apparatus. The heating block possesses 3 capillary tube holders. The heating rate was set at 0.5 °C min^{-1}.

2. Synthesis and Characterisation

The azobenzene photosurfactant tetraethylene glycol mono(4',4-octyloxy, octyl-azobenzene ($C_8AzoOC_8E_4$) was synthesised in three main stages: (1) the preparation of a hydroxyl precursor; (2) modification to a bromoprecursor; (3) addition of the polar tetraethylene glycol head group to form the final AzoPS**.** All intermediates and products were characterised by ^{1}H and ^{13}C NMR spectroscopy, FTIR spectroscopy, mass spectrometry and melting point analysis.

Synthesis of hydroxyl precursor, 4-octyl-4'-hydroxyl azobenzene: In a 250 mL round-bottom flask, 4-octylaniline (20 mmol, 4.57 mL) was dissolved in an acetone:water mixture (1:1, 50 mL) with HCl (37.5%, 0.048 mol, 4 mL) and stirred for 20 min in an ice bath. Separately, $NaNO_2$ (1.7 g, 20 mmol) was dissolved in distilled H_2O (25 mL) and cooled to 1-3 °C. To the cooled 4-octylaniline solution, the $NaNO_2$ solution was added slowly, and left for 20 min to stir in an ice bath to produce the diazonium salt. Additionally, phenol (1.9 g, 20 mmol), NaOH (0.8 g, 20 mmol) and Na_2CO_3 (2.1 g, 20 mmol) were dissolved in distilled H_2O (50 mL), stirred for 5 min and cooled to 1-3 °C. To this solution, the resultant diazonium salt was added dropwise and the temperature was maintained below 8 °C. An aqueous NaOH solution (6.5 mL, 2.5 mmol L^{-1}) was added dropwise to the basic phenol solution along with the acidic diazonium salt solution, to maintain a final pH of 10. The resulting orange precipitate was left to warm to room temperature, filtered and washed with cold distilled water. **C_8AzoOH** was recovered as an orange powder in 70% yield.

^{1}H NMR: ($CDCl_3$, 400 MHz, 25 °C): δ = 0.90 (t, *J* = 7 Hz, 3H), 1.33 (m, 8H), 1.66 (m, 4H), 2.69 (t, *J* = 7 Hz, 2H), 5.5 (s, br.,), 6.96 (d, *J* = 7.2 Hz, 2H), 7.32 (d, *J* = 9 Hz, 2H), 7.81 (d, *J* = 7.2 Hz, 2H), 7.88 (d, *J* = 8.4 Hz, 2H) ppm.

^{13}C NMR: ($CDCl_3$, 100 MHz, 25 °C): δ = 14.2, 22.7, 29.3, 29.5, 31.3, 31.9, 35.9, 115.9, 122.5 125.1, 129.1, 146.1, 147.1, 150.6, 158.3 ppm.

FTIR: *v* = 3427 (br), 2956 (s), 2923 (s), 2856 (s), 1586 (s), 1465 (s), 1243 (s), 1135 (s), 833 (s), 558 (s) cm^{-1}.

Mass Spectrometry (CH_3Cl, m/z: $APCI^+$): Exact mass calculated: 310.2045 [M], exact mass obtained: 309.1977 $[M-H]^+$.

Melting Point: 87.2 – 88.8 °C.

Synthesis of bromoprecursor, 4-octyl-4'(8-bromo)octyloxy azobenzene: C_8AzoOH (1 eq., 10 mmol, 3 g), was dissolved in acetone (50 mL). 1,8-dibromooctane (2 eq., 20 mmol, 3.68 mL), K_2CO_3 (2 eq., 20 mmol, 2.76 g) and KI (0.1 eq., 1 mmol, 0.17 g) were added to the reaction flask and the resulting dark red solution was stirred under reflux at 65 °C for 2 days. Acetone was removed *via* rotary evaporation and the product was dissolved in dichloromethane (DCM, 20 mL) and washed with water several times to remove the co-salt. DCM was removed *via* rotary evaporation and **C_8AzoOC_8Br** was recovered as an orange solid in 80% yield upon recrystallisation from ethanol.

^{1}H NMR: ($CDCl_3$, 400 MHz, 25 °C): δ = 0.91 (t, *J* = 8 Hz, 3H), 1.29-1.35 (m, 10H), 1.4 – 1.47 (m, 8H), 1.66 (quint., 2H), 1.86 (m, 4H), 2.69 (t, *J* = 7 Hz, 2H), 3.44 (m, 2H), 4.05 (t, *J* = 7 Hz, 2H), 7.01 (d, *J*= 9 Hz, 2H), 7.32 (d, *J* = 8.5 Hz, 2H), 7.81 (d, *J* = 8.6 Hz, 2H), 7.9 (d, *J* = 8.7 Hz, 2H) ppm.

^{13}C NMR: ($CDCl_3$, 100 MHz, 25 °C): δ = 14.1, 26, 29.2, 28.1, 28.5, 28.6, 28.7, 29.3, 29.3, 29.5, 31.4, 31.9, 32.7, 33.9, 35.9, 68.3, 114.7, 122.5, 124.6, 129.1, 145.8, 147, 151.1, 161.4 ppm.

FTIR: *v* = 2983 (s), 2916 (s), 2849 (s), 1600 (s), 1492 (s), 1470 (s), 1256 (s), 1122 (s), 833 (s), 550 (s) cm^{-1}.

Mass Spectrometry (CH_3Cl, m/z: $APCI^+$): Exact mass calculated: 500.2402 [M], exact mass obtained: 501.2473 $[M+H]^+$.

Melting Point: 119.8 - 121.2 °C

Synthesis of tetraethylene glycol mono(4',4-octyloxy, octyl-azobenzene: Tetraethylene glycol (5 eq., 28.1 mmol, 5.41 mL) was dried azeotropically by distillation with toluene (20 mL) at 170 °C. Dry tetraethylene glycol was then dissolved in dry THF (25 mL) in a round-bottomed flask (50 mL) under an inert N_2 atmosphere. To this NaH (60% in oil (w/w), 1.5 eq., 8.4 mmol, 0.346 g) was added and left to stir for 1 h under N_2. C_8AzoOC_8Br (1.0 eq, 5.6 mmol, 2.8 g) was dissolved in dry THF (10 mL) and added to the reaction flask. The resulting red solution was refluxed at 65 °C for 24 h. THF was removed *via* rotary evaporation and the resulting red oil dissolved in DCM (20 mL) and washed with water. The DCM layer was dried using $MgSO_4$, filtered and the solvent was removed *via* rotary evaporation. Excess bromoprecursor was removed using a silica plug and washing with chloroform. The product was recovered with acetone and the solvent removed *via* rotary evaporation to yield $C_8AzoOC_8E_4$ as a red oil in 47% yield.

^{1}H NMR: ($CDCl_3$, 400 MHz, 25°C): δ = 0.84 (t, *J* = 8 Hz, 3H), 1.26 – 1.54 (m, 24H), 1.78 (m, 2H), 2.63 (t, *J* = 8 Hz, 2H), 3.64 (m, 16 H), 3.99 (t, *J* = 7 Hz, 2H), 6.95 (d, *J* = 9 Hz, 2H), 7.25 (d, *J* = 8.32 Hz, 2H), 7.75 (d, *J* = 8.36 Hz, 2H), 7.84 (d, *J* = 8.96 Hz, 2H) ppm.

^{13}C NMR: ($CDCl_3$, 600 MHz, 25°C): δ = 14.06, 22.61, 25.93, 29.2, 29.3, 29.2, 29.3, 29.3, 29.3, 30.9, 31.3, 31.8, 33.6, 35.8, 61.5, 68.3, 70.2-70 (7 peaks), 72.8, 114.6, 122.5, 124.5, 129, 145.8, 146.9, 151, 161.1 ppm.

FTIR: *v* = 3169 (br.), 2971 (w), 2928 (m), 2867 (w), 1594 (s), 1498 (s), 1247 (s), 1139 (s) cm^{-1}.

Elemental Analysis: Found: 68.0 % C, 9.7% H, 4.1% N. Calculated for $C_{36}H_{58}N_2O_6$: 70.3% C, 9.5% H, 4.5% N (>97% purity).

Mass Spectrometry (CH_3Cl, m/z: $APCI^+$): Exact mass calculated: 614.4295 [M]. Exact mass obtained: 615.4390 $[M+H]^+$.

3. Photostability of Azobenzene Cycling

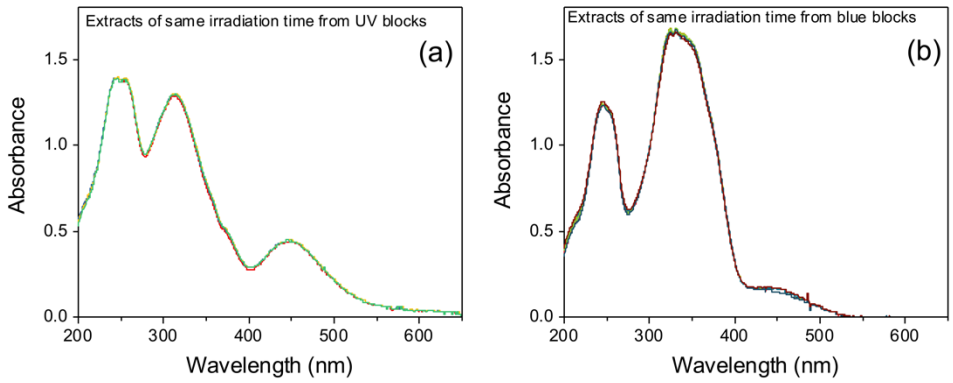

Figure S1. $C_8AzoOC_8E_4$ is robust and can isomerise reversibly over several hours with no deterioration. UV-Vis absorption spectra of $C_8AzoOC_8E_4$ in D_2O (0.2 mmol L^{-1}) (a) measured for a fixed UV irradiation time (365 nm) and (b) for a fixed blue light irradiation time (450 nm). Both sets of spectra were recorded during the repeated cycling of UV and blue irradiations, which were necessary to improve statistics in the SANS experiments.

4. Photoisomerisation Studies

4.1 Determination of the Degree of Isomerisation

The degree of isomerisation in the *cis*-photostationary state can be calculated from the ratio of the *cis*-PSS absorbance to 100% *trans*-isomer absorbance, at a given wavelength:[1]

$$ID_{trans-cis} = \frac{A(0)_{350} - A(PSS)_{350}}{A(0)_{350}} \times 100\% \qquad \text{Eq. S1}$$

where $A(0)_{350}$ refers to the absorbance of the assembly of 100% *trans*-isomers at 350 nm and $A(PSS)_{350}$ refers to the absorbance of the *cis*-PSS at 350 nm. For *cis*-$C_8AzoOC_8E_4$, $ID_{trans\text{-}cis}$ = 61%. Similarly, for reverse isomerisation, a majority *trans*-PSS is obtained. The degree of isomerisation in this case can be calculated in an analogous manner to that for the *cis*-PSS:

$$ID_{cis-trans} = \frac{A(PSS)_{350}}{A(0)_{350}} \times 100\% \qquad \text{Eq. S2}$$

where $A(0)_{350}$ still refers to the absorbance of the assembly of 100% *trans*-isomers at 350 nm and $A(PSS)_{350}$ now refers to the absorbance of the *trans*-PSS at 365 nm. $ID_{cis\text{-}trans}$ was found to be 90% for *trans*-$C_8AzoOC_8E_4$.

4.2 Degree of Isomerisation for *in-situ* Measurements

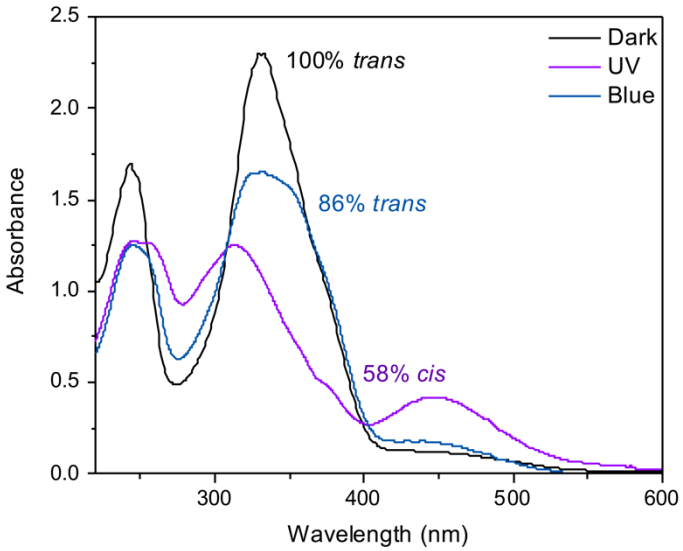

Figure S2. UV-Vis absorption spectra of $C_8AzoOC_8E_4$ (0.2 mmol L^{-1}) after 10 min UV (purple line) and 10 min blue (blue line) irradiation and after dark storage (black line).

5 Small-Angle Neutron Scattering Data and Fitting

5.1 Structural Parameters from SANS Model Fitting

Table S1. Structural parameters obtained from SANS data for $C_8AzoOC_8E_4$ under blue light illumination in D_2O (0.2 mmol L^{-1}) at 25 °C. When deconvolution into two models is required, dark grey boxes refer to the flexible elliptical cylinder (FEC) model while the light grey boxes refer to the elliptical cylinder model (EC). L_c is the contour length, L_k is the Kuhn length, L_{cyl} is the cylinder length, r_m is the minor axis radius, a_r is the axis ratio, SLD refers to the scattering length density, χ^2 gives an indication of the goodness of fit and X_{sol} is the calculated solvent fraction of the aggregates.

Time (s)	Model	L_c	b (Å)	SLD ($\times10^{-6}$ Å^{-2})	χ^2	X_{sol}	L_{cyl} (Å)	r_m (Å)	a_r	SLD ($\times10^{-6}$ Å^{-2})	χ^2	X_{sol}
60	FEC	*	211.7	5.3	1.9	0.82	-	29.5	15.6	-	-	-
120	FEC	*	222.2	5.4	1.7	0.84	-	27.1	18.3	-	-	-
180	FEC	*	356.1	5.5	4.3	0.85	-	27.7	19.3	-	-	-
240	FEC	*	648.0	5.7	7.1	0.89	-	30.2	19.5	-	-	-
300	FEC/EC	*	243.9	5.7	0.7	0.89	366.8	32.2	5.1	5.3	2.7	0.82
360	FEC/EC	*	405.0	5.3	1.3	0.82	397.4	33.5	5.4	5.1	2.4	0.79
420	FEC/EC	*	636.2	5.7	1.8	0.89	615.0	34.4	5.1	5.1	2.2	0.79
480	FEC/EC	*	481.8	5.3	1.5	0.82	488.9	35.0	5.8	5.2	2.0	0.80
540	FEC/EC	*	446.0	5.3	1.2	0.82	589.2	36.1	5.7	5.0	1.7	0.77

* values for L_c lay outside the observation window of this experiment and are therefore not reported.

Table S2. Structural parameters obtained from SANS data for $C_8AzoOC_8E_4$ under UV light illumination in D_2O (0.2 mmol L^{-1}) at 25 °C. When deconvolution into two models is required, dark grey boxes refer to the flexible elliptical cylinder (FEC) model while the light grey boxes refer to the elliptical cylinder model (EC). L_c is the contour length, L_k is the Kuhn length, L_{cyl} is the cylinder length, r_m is the minor axis radius, a_r is the axis ratio. For the fractal model, V_{fr} refers to the volume fraction, r is the radius of the constituent components, D is fractal dimension, L_{corr} is the correlation length. In all cases, SLD refers to the scattering length density, χ^2 gives an indication of the goodness of fit and X_{sol} is the calculated solvent fraction of the aggregates.

Time (s)	Model	L_c	L_K (Å)	SLD ($\times10^{-6}$ Å^{-2})	χ^2	X_{sol}	L_{cyl} (Å)	r_m (Å)	a_r	SLD ($\times10^{-6}$ Å^{-2})	χ^2	X_{sol}
60	FEC/EC	*	517.7	5.1	7.3	0.79	587.7	41.2	5.7	4.8	7.8	0.73
120	FEC/EC	*	328.0	5.5	2.6	0.85	460.0	24.8	7.5	5.0	2.1	0.77
180	FEC/EC	*	711.0	5.1	2.3	0.79	446.4	22.1	9.2	4.5	2.5	0.68
240	-	-	-	-	-	-	-	-				
300	-	-	-	-	-	-	-	-				
		V_{fr}	r (Å)	SLD ($\times10^{-6}$ Å^{-2})	χ^2	X_{sol}	L_{corr} (Å)	D				
360	fractal	0.40	44.0	4.5	7.5	0.68	917.3	2.53				
420	fractal	0.37	44.0	4.7	7.4	0.71	755.5	2.56				
480	fractal	0.41	43.4	5.1	7.3	0.79	1856	2.56				
540	fractal	0.36	42.4	5.5	6.7	0.85	1057	2.50				

5.2 Intensities of Scattering Profiles

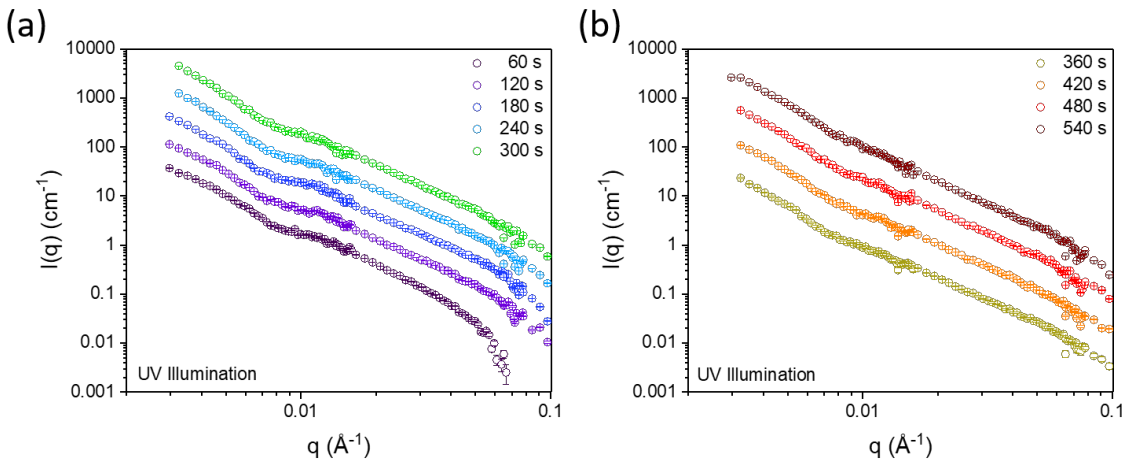

Figure S3. SANS scattering profiles of $C_8AzoOC_8E_4$ (0.2 mM in D_2O) as a function of UV irradiation time. (a) from 60 to 300 s of UV irradiation. Graphs are offset by a factor of 5, 25, 100, and 400, respectively. (b) from 360s to 540 s. Graphs are offset by a factor of 5, 25 and 100, respectively.

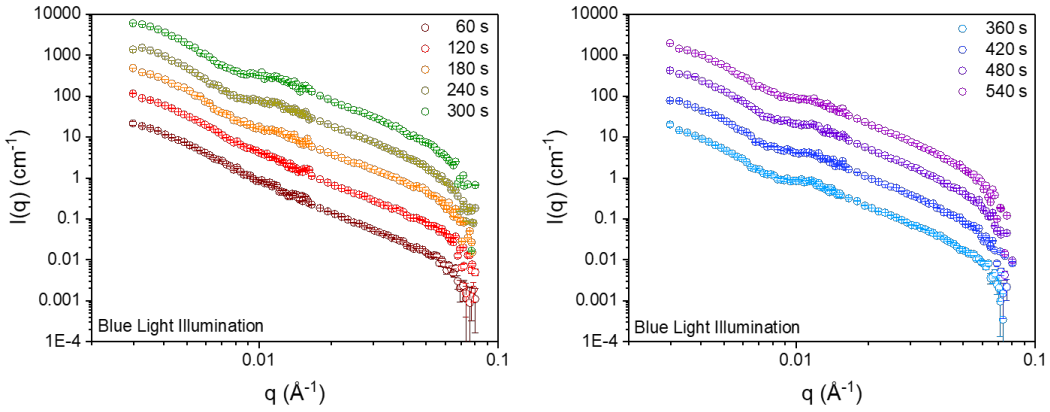

Figure S4. SANS scattering profiles of $C_8AzoOC_8E_4$ (0.2 mM in D_2O) as a function of blue light irradiation time. (a) from 60 to 300 s of UV irradiation. Graphs are offset by a factor of 5, 25, 100, and 400, respectively. (b) from 360s to 540 s. Graphs are offset by a factor of 5, 25 and 100, respectively.

5.3 Comparison of Flexible Elliptical Cylinder Models

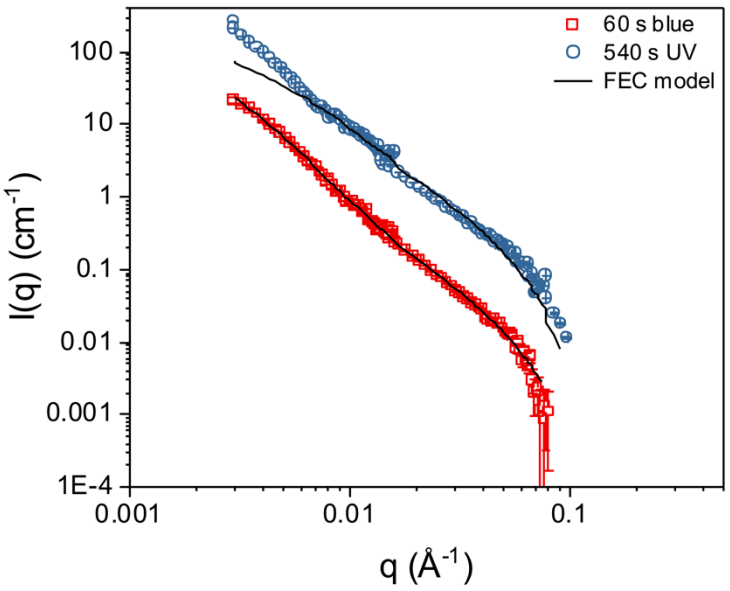

Figure S5. SANS scattering profiles of $C_8AzoOC_8E_4$ after 60 s blue (red line) and 540 s UV (blue line) illumination. The black solid line indicates a fit to a flexible elliptical cylinder (FEC) model. The UV scattering curve has been offset by a factor of 10 for clarity.

5.4 Comparison of the Intensity of Small-Angle Neutron Scattering

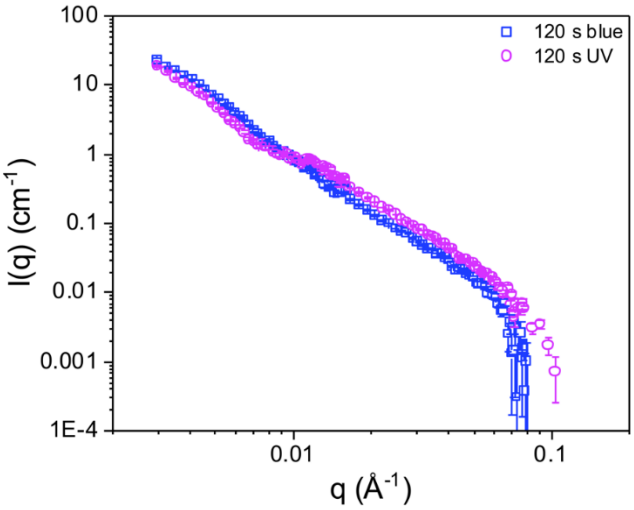

Figure S6. SANS scattering profiles of $C_8AzoOC_8E_4$ after 120 s of blue (blue line) and UV (pink line) irradiation. The scattering intensity is comparable for both.

5.5 SANS Profiles at Equilibrium (0.2 mmol L^{-1})

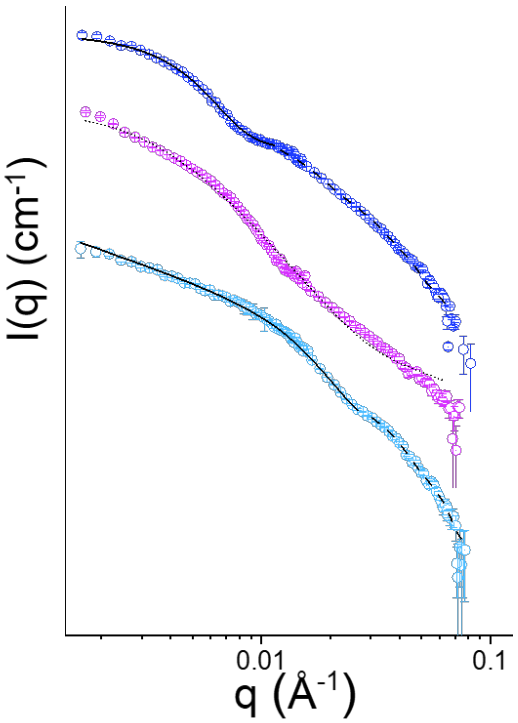

Figure S7. SANS profiles of $C_8AzoOC_8E_4$ (0.2 mmol L^{-1} in D_2O) in the native *trans*-dominant state (teal), and in the *cis*- (pink) and *trans*-PSS (blue) after UV and blue irradiation, respectively. Fits to a flexible elliptical cylinder model are shown with a black line, fits to an elliptical cylinder model with a dashed line and fits to the fractal model are shown with a dotted line. The scattering profiles have been offset for clarity.

Table S3. Structural parameters obtained from SANS data for $C_8AzoOC_8E_4$ in the *trans*-dominant native state, and *cis* and *trans* PSS in D_2O (0.2 mmol L^{-1}) at 25 °C. When deconvolution into two models is required, dark grey boxes refer to the flexible elliptical cylinder (FEC) model while the light grey boxes refer to the elliptical cylinder model (EC). L_c is the contour length, L_k is the Kuhn length, L_{cyl} is the cylinder length, r_m is the minor axis radius, a_r is the axis ratio. For the fractal model, V_{fr} refers to the volume fraction, r is the radius of the constituent components, D is fractal dimension, L_{corr} is the correlation length. In all cases, SLD refers to the scattering length density, χ^2 gives an indication of the goodness of fit and X_{sol} is the calculated solvent fraction of the aggregates.

	Model	L_K (Å)	SLD ($\times10^{-6}$ Å^{-2})	χ^2	X_{sol}	L_{cyl} (Å)	r_m (Å)	a_r	SLD ($\times10^{-6}$ Å^{-2})	χ^2	X_{sol}
trans native	FEC/EC	259.4	5.3	1.8	0.82	260.0	42.1	20.5	5.2	0.9	0.80
trans-PSS	FEC/EC	476.9	5.5	1.2	0.84	342.6	42.6	3.6	5.4	1.7	0.85

		V_{fr}	SLD ($\times10^{-6}$ Å^{-2})	r (Å)	χ^2	X_{sol}	L_{corr} (Å)	D
cis-PSS	Fractal	0.2	4.0	26.2	32.0	0.59	246	3

5.6 SANS Profiles at Higher Concentration (1 mmol L^{-1}).

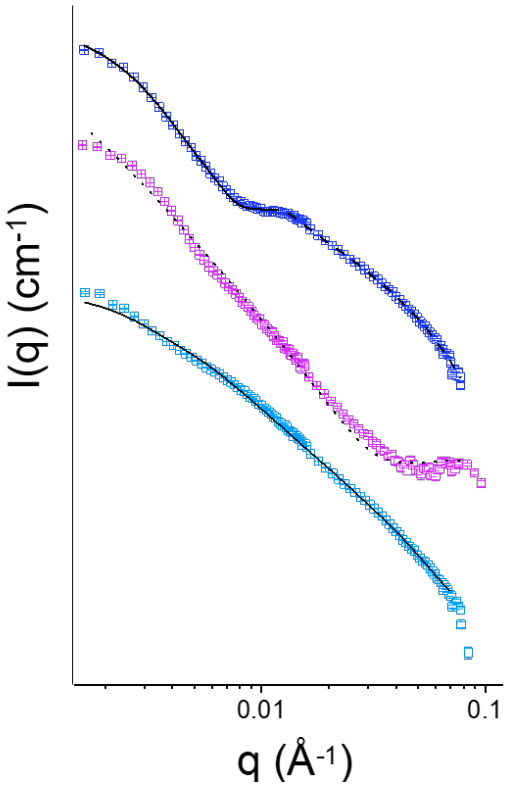

Figure S8. SANS profiles of $C_8AzoOC_8E_4$ (1 mmol L^{-1} in D_2O) in the native *trans*-dominant state (teal), and in the *cis*- (pink) and *trans*-PSS (blue) after UV and blue irradiation, respectively. Fits to a flexible elliptical cylinder model are shown with a black line, fits to an elliptical cylinder model with a dashed line and fits to the fractal model are shown with a dotted line. The scattering profiles have been offset by a factor of 10 for clarity.

Table S4. Structural parameters obtained from SANS data for $C_8AzoOC_8E_4$ in the *trans*- dominant native state, and *cis* and *trans* PSS in D_2O (1 mmol L^{-1}) at 25 °C. When deconvolution into two models is required, dark grey boxes refer to the flexible elliptical cylinder (FEC) model while the light grey boxes refer to the elliptical cylinder model (EC). L_c is the contour length, L_k is the Kuhn length, L_{cyl} is the cylinder length, r_m is the minor axis radius, a_r is the axis ratio. For the fractal model, V_{fr} refers to the volume fraction, r is the radius of the constituent components, D is fractal dimension, L_{corr} is the correlation length. In all cases, SLD refers to the scattering length density, χ^2 gives an indication of the goodness of fit and X_{sol} is the calculated solvent fraction of the aggregates.

	Model	L_K (Å)	SLD ($\times10^{-6}$ Å^{-2})	χ^2	X_{sol}	L_{cyl} (Å)	r_m (Å)	a_r	SLD ($\times10^{-6}$ Å^{-2})	χ^2	X_{sol}
trans native	FEC	190.0	5.5	4.0	0.85	-	39.4	5.0	-	-	
trans-PSS	FEC/EC	304.0	5.5	2.3	0.85	366.2	34.0	4.5	4.7	3.0	0.71

		V_{fr}	SLD ($\times10^{-6}$ Å^{-2})	r (Å)	χ^2	X_{sol}	L_{corr} (Å)	D
cis-PSS	Fractal	0.5	4.2	60.0	6.0	0.63	1762.2	3

6. Calculation of the Packing Parameter

The morphology of the self-assembled structure formed can be predicted using the concept of a packing parameter, $P = V/a_e l_c$, where V is volume of the hydrophobic tail, a_e is the area occupied by headgroups at the hydrophilic-hydrophobic interface, and l_c is the length of the hydrocarbon tail. A packing parameter of $1/3 < P < 1/2$ indicates the formation of cylindrical micelles. Values for V and l_c were calculated by the empirical volume additivity rule of Traube:[2]

$$V = \sum V_i \qquad \text{Eq. S3}$$

$$l_c = \sum l_{ci} \qquad \text{Eq. S4}$$

where V_i and l_{ci} are the contributions of the ith components. The calculated value for the packing parameter of $C_8AzoOC_8E_4$ using this general approach and the methods outlined in Table S3 is $P = 0.42$.

Table S5 Contribution of volumes, lengths and effective area to calculate the packing parameter, *P*.

Contributions	Values	Method
Alkyl chain volume (nm^3)	0.0269*m* + 0.0274	Tanford equations[3]
Azobenzene volume (nm^3)	0.176/0.177 (*trans*/*cis*)	MOPAC calculations, van der Waals volume[6]
Oxy-group volume (nm^3)	9.1×10^{-3}	*Ab initio* calculations, van der Waals volume[2]
Alkyl chain length (nm)	0.1265*m* + 0.15	Tanford equations[3]
Azobenzene length (nm)	0.9/0.55 (*trans*/*cis*)	From X-Ray analysis[5]
Oxy-group length (nm)	0.28	DFT calculations[4]
E_4 effective area (nm^2)	0.46	ST study of $C_{12}E_4$ at 25 °C[7]

7. Rheology Data

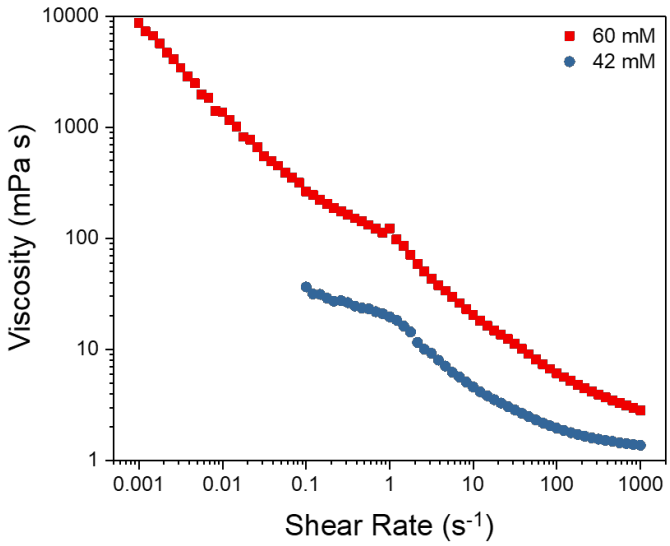

Figure S9. Viscosity sweep of *trans*-C_8AzoOC_8E_4 in water at 42 mM (blue) and 60 mM (red) at 25 °C. The surfactant solution has a high viscosity compared to water (0.89 mPa s) and exhibits non-Newtonian shear thinning behaviour, with the viscosity decreasing as the shear rate increases. These two characteristics are commonly observed for wormlike micelle systems.

8. References

1 S. Peng, Q. Guo, P. G. Hartley and T. C. Hughes, *J. Mater. Chem. C*, 2014, **2**, 8303–8312.

2 H. Durchschlag, P. Zipper, in *Ultracentrifugation* (Ed.: M. D. Lechner), Steinkopff, Darmstadt, **1994**, pp. 20-39.

3. C. Tanford, *J. Phys. Chem.* **1972**, *76*, 3020-3024.

4. F. Agapito, B. J. C. Cabral, J. A. M. Simões, *Journal of Molecular Structure: THEOCHEM* **2005**, *719*, 109-114.
5. E. Merino, M. Ribagorda, *Beilstein J. Org. Chem.* **2012**, *8*, 1071-1090.
6. K. Takeshita, N. Hirota, M. Terazima, *J. Photochem. Photobiology A: Chem.* **2000**, *134*, 103-109.
7. M. J. Rosen, A. W. Cohen, M. Dahanayake, X. Y. Hua, *J. Phys. Chem.* **1982**, *86*, 541-545